



Proceedings of the Seventeenth International Conference on  
Civil, Structural and Environmental Engineering Computing  
Edited by: P. Iványi, J. Kruis and B.H.V. Topping  
Civil-Comp Conferences, Volume 6, Paper 13.1  
Civil-Comp Press, Edinburgh, United Kingdom, 2023  
doi: 10.4203/ccc.6.13.1  
©Civil-Comp Ltd, Edinburgh, UK, 2023

## **A Bistable SMA Actuator: Design and Analysis**

**M. Battaglia, A. Sellitto, V. Acanfora  
and A. Riccio**

**Department of Engineering,  
University of Campania “Luigi Vanvitelli”,  
Aversa, Italy**

### **Abstract**

Bistable shape memory alloy (SMA) actuators have gained significant attention due to their ability to maintain stable positions without requiring a continuous supply of power. This feature is particularly advantageous in applications where power consumption is a concern, as it allows for efficient energy usage and reduced operating costs. In addition, bistable SMA actuators have a fast response time and high force output, making them suitable for a wide range of applications in fields such as robotics, aerospace, and biomedical engineering. The unique properties of SMA materials, including the shape memory effect and superelasticity, provide numerous benefits for actuator design and operation. The present research introduces the design of a bistable actuator that utilizes shape memory alloys (SMA) to generate high forces while maintaining a compact and lightweight form factor.

**Keywords:** bistable actuator, shape memory alloys, SMA Actuator, finite element method

### **1. Introduction**

In recent years, there has been an increasing demand for intelligent systems with high-performance functionality [1,2]. Therefore, there is a continuous need for compact

and high-performance actuators that can meet stringent performance and weight requirements [3-5].

Actuators used to be a concern due to the increased mass on the component. Common pneumatic and hydraulic actuators are extremely heavy and have a large footprint as well. In numerous engineering fields, such as aerospace and automotive, mass is a critical factor that exerts a significant impact [6]. Excessive weight of components can have adverse effects on fuel consumption and cost, necessitating continuous improvement in this regard. Therefore, it is important to explore alternative technologies that can meet both thermal and mechanical requirements while minimizing size and weight. Shape memory alloy (SMA) actuators have been the subject of various studies, and have been found to possess desirable characteristics in a wide range of applications, including aerospace, automotive, biomedical, and civil engineering [7-9].

One of the main benefits of a bistable shape memory alloy (SMA) actuator is its ability to maintain its position without requiring a continuous supply of power [10,11]. The actuator's inherent bistability enables it to maintain either of its stable positions without requiring an external force to hold it in place. The feature renders the actuator highly useful for applications where power consumption is a critical consideration, as it allows the actuator to sustain a position or support a load with minimal energy input. Shape memory alloys (SMA) are a popular choice for actuators due to their unique properties, including the shape memory effect and superelasticity. In recent years, numerous studies have been conducted to investigate shape memory alloys, which belong to the category of "smart materials" [12,13]. Shape memory alloys (SMAs) have the ability to restore their original shape after being subjected to either mechanical or thermal loads. This is attributed to their capacity to alter their crystalline structure in response to applied deformation. The alloys exhibit two distinct effects, namely the pseudo-elastic effect and the shape memory effect [14,15]. The first concerns the ability of the alloy to return to its unformed configuration after the application of mechanical load. The second concerns the material's ability to thermally 'recover' the undeformed configuration after partial recovery of residual deformation. Once the load applied to the material exceeds the threshold value that triggers the phase transition, the material will undergo a gradual change in shape that follows a plateau. This plateau is primarily influenced by the volumetric fraction of martensite and serves to regulate the material's transformation behaviour [16]. The two crystalline phases of shape memory alloys are austenite and martensite. The former is stable at high temperatures and low stresses, the latter is stable at low temperatures and high stresses. Again, by cooling austenite, it is possible to have two different phases of martensite. The first, the one mentioned earlier, is stable with temperature, the second, the R-phase forms, having a low activation energy, forms earlier and therefore have an energy advantage [17].

The objective of this study is to develop a bistable actuator that satisfies demanding specifications for strength while also minimizing space requirements. To achieve this goal, the actuator employs shape memory alloys as the primary technology for

actuation. The issue of direct current is addressed in this study, resulting in a solution that not only reduces energy consumption but also prevents the deterioration of the alloys themselves.

In Section 2, a Shape Memory Alloy overview is presented. In section 3, a description of a bistable SMA actuator is provided. In section 4 the analysis of the bistable actuator and an in-depth discussion of the thermo-mechanical behaviour of SMA springs is introduced and commented. Conclusions are reported in section 5.

## 2. Shape Memory Alloy overview

Shape memory alloys are metal alloys capable of recovering their shape after applying a mechanical or thermal load. The pseudo-elastic and shape memory effect makes them particularly suitable for use in engineering as actuators.

To conduct a numerical simulation of the thermomechanical behaviour of SMA materials using User subroutine MATerial, only a subset of the characteristic parameters of these alloys are utilized. Regarding temperatures, four specific temperatures can be established to delineate the crystalline phase alteration of the alloy, namely Ms, Mf, As, and Af.

- Ms: martensite start transformation.
- Mf: martensite finish transformation.
- As: austenite start transformation.
- Af: austenite finish transformation.

Temperatures are related to mechanical behaviour as illustrated in Figure 1. Once the reference temperature has been set, the characteristic phase change stresses are determined:  $\sigma_M^S$ ,  $\sigma_M^f$ ,  $\sigma_A^S$ ,  $\sigma_A^f$ .

- $\sigma_M^S$ : martensite start transformation stress.
- $\sigma_M^f$ : martensite finish transformation stress.
- $\sigma_A^S$ : austenite start transformation stress.
- $\sigma_A^f$ : austenite finish transformation stress.

In the  $(\sigma, T)$  diagram, the band slope corresponds to the forward and reverse phase transformations, with  $C_A$  and  $C_M$  representing the band slope for the forward and reverse transformations. The critical stress values for the start and end of the austenite to martensite phase transformation are  $\sigma_{scr}$  and  $\sigma_{fer}$ .

The phase change is relevant as it is linked to a change in material stiffness that affects the response of the SMA structure. According to an experimental study made by Petr Šittner et al., the Martensite phase has a lower stiffness ( $E_M$ ) than austenite ( $E_A$ ) due to the combination of elastic anisotropy of the B19' martensite and strong martensite [18].

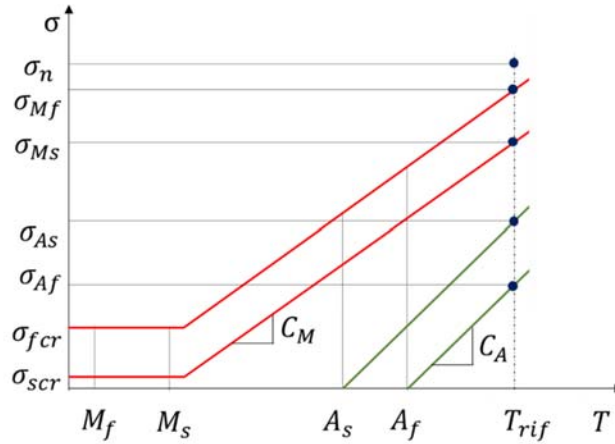


Figure 1:  $\sigma$ - $T$  diagram phase.

The unique physical and thermal properties of shape memory alloys, along with their capability to undergo phase changes that affect their stiffness, render them highly suitable for a diverse range of applications. Moreover, the combination of their pseudoelastic and shape memory effects make them an excellent choice for actuation purposes. Figure 2 illustrates the pseudoelastic effect. If the reference temperature is greater than the  $A_f$  temperature, the material can regain its original shape without requiring the application of a thermal load to reverse deformation.

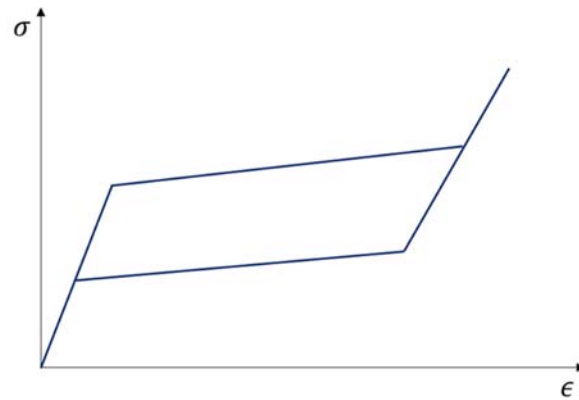


Figure 2: Pseudoelastic effect.

When the reference temperature is lower than the  $A_f$  temperature, the material is not able to recover residual strain, so the application of thermal load is required to have zero residual strain (Figure 3).

### 3. SMA Actuator

SMA actuators are very efficient in terms of exerted forces and low mass. According to a study by Mohd Jani et al. [19], SMA actuators have 200% more work per volume than hydraulic actuators and 150% more power per volume.

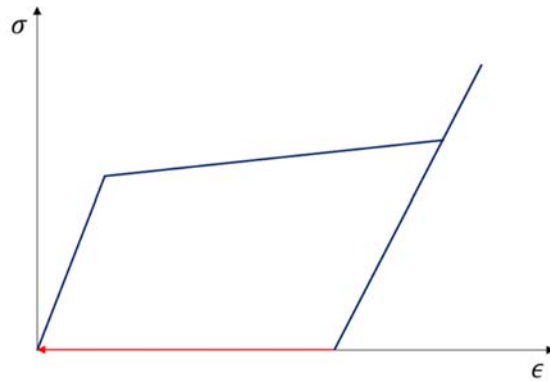


Figure 3: Shape memory effect.

Generally, they have a low efficiency compared to other actuators, as they have a low actuation frequency and low controllability. In addition, they need continuously applied current to be activated. Furthermore, to reduce time, heating takes place in very short times with high currents that deteriorate the material [20-22]. To overcome some of the limitations listed above, a bistable actuator has been designed (Figure 4). This approach mitigates the likelihood of material degradation, as it does not depend on continuous electrical input. Furthermore, it notably enhances the cooling process [23].

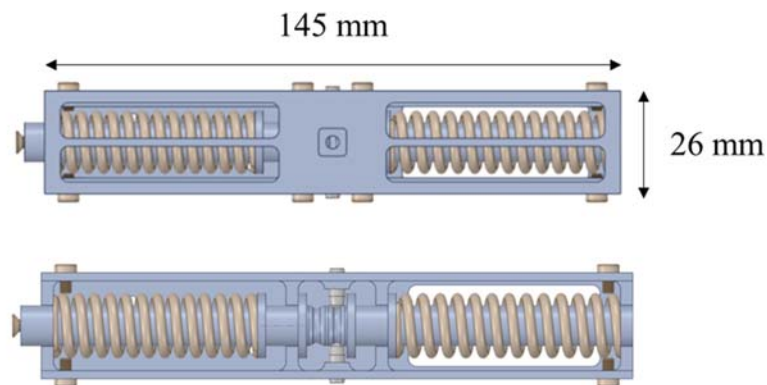


Figure 4: SMA Actuator.

The actuator consists of a central body, two SMA springs working in phase opposition, two blocking springs, and an outer case. The components of the system that remain fixed include the external case, which serves to connect with external parts, the blocking springs designed with a stiffness of 7 N/mm, and the external segments of the SMA springs that are confined to fit within the case.

The two SMA springs are previously precompressed 55mm at a temperature of 298 K. At this temperature, the springs cannot recover all the residual deformation and therefore a thermal load of 100°, alternately on one or the other spring, is required for activation. The object that moves due to the thrust of the SMA spring is the central

body, which slides along the longitudinal direction for a maximum of 5 mm (actuator stroke). Upon passing the initial position, the central body is secured in the second position with the assistance of two locking springs that exceed the force of the SMA springs (Figure 5).

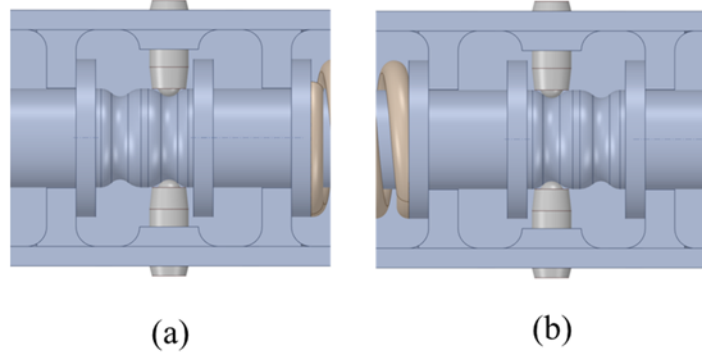


Figure 5: Bistable actuator. (a) First stable positions; (b) Second stable positions.

#### 4. Results

To simulate both effects of shape memory alloys, it has been necessary to use a User subroutine MATerial (UMAT). This made it possible to study the behaviour of the alloy in the martensitic phase, in the austenitic phase and in the plateau phase. The routine is able to define, inside the numerical model, the volume fraction of martensite (the value that defines how much of the austenite has turned into martensite). This value is of great significance, as it serves as an indicator of how well the spring is optimized with respect to the required force and whether its shape can be further optimized to enhance performance.

The thermal and mechanical properties of NiTiNOL were obtained by internal testing, the approach of which is similar from that reported in [24, 25].

<b>Nitinol</b>			
$\sigma_{scr}$ [MPa]	15	$\alpha_M$ [1/°K]	$2.2 \times 10^{-6}$
$\sigma_{fcr}$ [MPa]	100	$\alpha_A$ [1/°K]	$2.2 \times 10^{-6}$
$E_M$ [GPa]	51.87	$\epsilon_l$	0.05
$E_A$ [GPa]	115.87	$M_s$ [°K]	338
$C_M$ [MPa/°K]	8	$M_f$ [°K]	303
$C_A$ [MPa/°K]	8	$A_s$ [°K]	328
$\nu_M$	0.33	$A_f$ [°K]	381
$\nu_A$	0.33		

Table 1: NiTiNOL thermo-mechanical properties.

To evaluate the mechanical performance and force output of the springs, it has been necessary to conduct a preliminary analysis of the SMA spring using the UMAT. As previously stated, a precompression of 55 mm has been applied to one end of the spring while the other end has been clamped. Subsequently, the 55 mm load has been removed, so the spring is permitted to deform, recovering roughly 3% of the initial load. After the spring has been stabilized, a thermal load is applied, resulting in the recovery of 90% of the deformation and the exertion of a force of roughly 750 N. The behaviour of the spring is shown in Figure 6. The green area corresponds to the loading phase in which the spring reaches 55 mm and a force value of 200 N. During the unloading phase, in blue, the spring recovers 3 mm and a force value close to 200 N. During the heating phase, in red, the spring recovers 50 mm and exerts a force of 750 N.

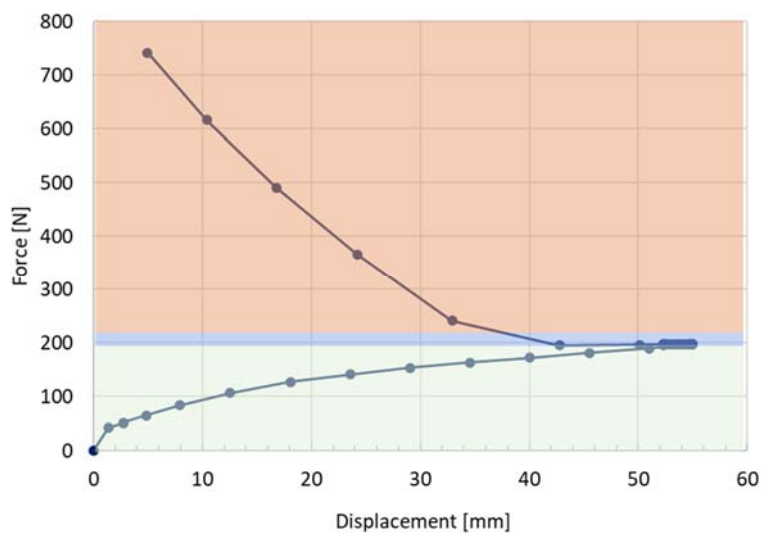


Figure 6: SMA spring. Force – displacement graph.

In Figure 7, the evolution of the volume fraction of martensite in the SMA spring (variable SDV7) is presented at different load step (spring unloaded at 298 K, spring fully preloaded at 298 K, spring unloaded and spring at 373 K).

According to Figure 7, the SMA spring has not undergone a complete transformation into martensite ( $\xi < 1$ ), this suggests that there is potential to enhance the spring's efficiency with respect to the specific load by optimizing its geometric features.

Regarding the complete dimensioning of the SMA actuator, seven numerical steps are necessary. The first step is referred to the compression of the two SMA springs. The second step is related to the compression of the two conventional springs. The unloading phase is in the third step. The fourth step is the heating of the first SMA spring. Then the cooling and the stabilisation. The seventh and the last step is the heating of the second SMA spring. The actuator, made of aluminium, shows no critical stresses. The maximum value occurs on the central part at the side of lateral springs (20 MPa). Figure 8 illustrates the movement of the actuator and the SMA springs. The

displacement is driven by the SMA springs, which push the actuator to move to the next equilibrium position.

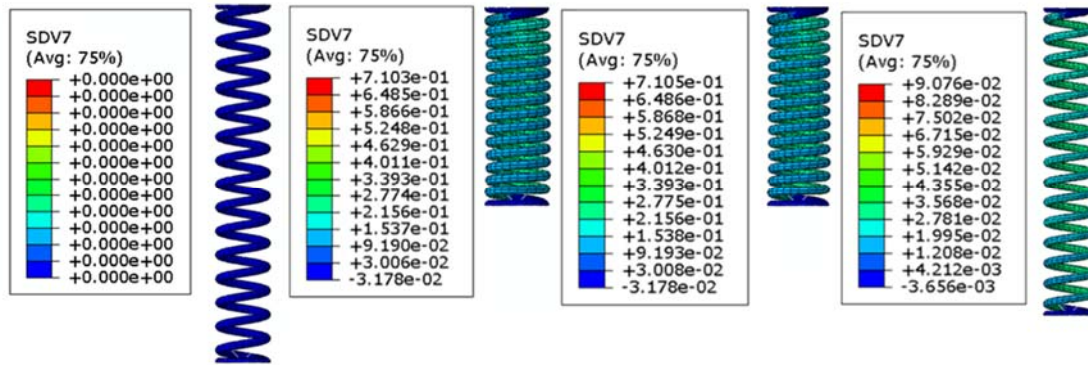


Figure 7: Volume fraction of martensite.

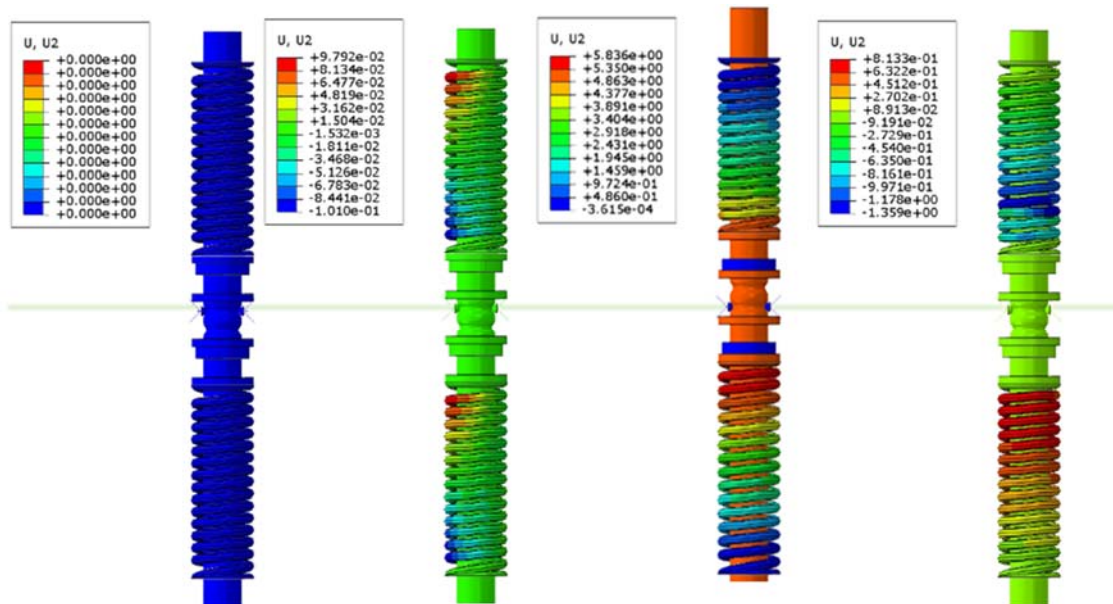


Figure 8: SMA actuator displacement.

## 5. Conclusions

The study's conclusions demonstrate the successful design of a bistable actuator based on shape memory alloys. The use of these alloys allowed for the development of an efficient actuator capable of providing high output forces with reduced energy consumption, thanks to the unique properties of shape memory alloys. Additionally, the actuator has been designed to be compact and lightweight, making it suitable for applications with limited space and weight.

## References

1. Liu, Y., Bao, R., Tao, J., Li, J., Dong, M., & Pan, C., Recent progress in tactile sensors and their applications in intelligent systems. *Science Bulletin*, 65(1), 70-88, 2020.
2. Hidalgo-López, J. A., Oballe-Peinado, Ó., Castellanos-Ramos, J., Sánchez-Durán, J. A., Fernández-Ramos, R., & Vidal-Verdú, F., High-accuracy readout electronics for piezoresistive tactile sensors. *sensors*, 17(11), 2513, 2017.
3. Solano, B., & Rotinat-Libersa, C., Compact and lightweight hydraulic actuation system for high performance millimeter scale robotic applications: modeling and experiments. *Journal of Intelligent Material Systems and Structures*, 22(13), 1479-1487, 2011.
4. Tsagarakis, N. G., Laffranchi, M., Vanderborght, B., & Caldwell, D. G., A compact soft actuator unit for small scale human friendly robots. In *2009 IEEE international conference on robotics and automation* (pp. 4356-4362). IEEE, 2009.
5. Hines, L., Petersen, K., Lum, G. Z., & Sitti, M., Soft actuators for small-scale robotics. *Advanced materials*, 29(13), 1603483, 2017.
6. Dimino, I., Ciminello, M., Concilio, A., Pecora, R., Amoroso, F., Magnifico, M., ... & Zivan, L., Distributed actuation and control of a morphing wing trailing edge. In *Smart Intelligent Aircraft Structures (SARISTU) Proceedings of the Final Project Conference* (pp. 171-186). Springer International Publishing, 2016.
7. Kohl, M., *Shape memory microactuators*. Springer Science & Business Media, 2004.
8. Mantovani, D., Shape memory alloys: Properties and biomedical applications. *Jom*, 52, 36-44, 2000.
9. Riccio, A., Sellitto, A., Ameduri, S., Concilio, A., & Arena, M. Shape memory alloys (SMA) for automotive applications and challenges. *Shape Memory Alloy Engineering*, 785-808, 2021.
10. Shao, H., Wei, S., Jiang, X., Holmes, D. P., & Ghosh, T. K., Bioinspired electrically activated soft bistable actuators. *Advanced Functional Materials*, 28(35), 1802999, 2018.
11. Cao, Y., Derakhshani, M., Fang, Y., Huang, G., & Cao, C., Bistable structures for advanced functional systems. *Advanced Functional Materials*, 31(45), 2106231, 2021.
12. Jani, J. M., Leary, M., Subic, A., & Gibson, M. A., A review of shape memory alloy research, applications and opportunities. *Materials & Design* (1980-2015), 56, 1078-1113, 2014.
13. Sellitto, A., & Riccio, A., Overview and future advanced engineering applications for morphing surfaces by shape memory alloy materials. *Materials*, 12(5), 708, 2019.
14. Lehnert, R., Müller, M., Vollmer, M., Krooß, P., Korpala, G., Prah, U., ... & Weidner, A., On the influence of crystallographic orientation on superelasticity-Fe-Mn-Al-Ni shape memory alloys studied by advanced in situ characterization techniques. *Materials Science and Engineering: A*, 871, 144830, 2023.

15. Omori, T., Ando, K., Okano, M., Xu, X., Tanaka, Y., Ohnuma, I., ... & Ishida, K., Superelastic effect in polycrystalline ferrous alloys. *Science*, 333(6038), 68-71, 2011.
16. Cao, B., & Iwamoto, T., An Experimental Study on Strain Rate Sensitivity of Strain-induced Martensitic Transformation in SUS304 by Real-time Measurement of Relative Magnetic Permeability. *steel research international*, 88(12), 1700022, 2017.
17. Duerig, T. W., & Bhattacharya, K., The influence of the R-phase on the superelastic behavior of NiTi. *Shape Memory and Superelasticity*, 1, 153-161, 2015.
18. Šittner, P., Heller, L., Pilch, J., Curfs, C., Alonso, T., & Favier, D., Young's modulus of austenite and martensite phases in superelastic NiTi wires. *Journal of materials engineering and performance*, 23, 2303-2314, 2014.
19. Jani, J. M., Leary, M., Subic, A., & Gibson, M. A., A review of shape memory alloy research, applications and opportunities. *Materials & Design (1980-2015)*, 56, 1078-1113, 2014.
20. Qiu J, Tani J, Osanai D, Urushiyama Y., High-speed actuation of shape memory alloy. *Smart Mater MEMS: Int Soc Opt Photonics* 2001:188–97.
21. Featherstone R, Teh Y., Improving the speed of shape memory alloy actuators by faster electrical heating. In: Ang Jr M, Khatib O, editors. *Experimental robotics IX*. Berlin Heidelberg: Springer; p. 67–76, 2006.
22. Chee Siong L, Yokoi H, Arai T., New shape memory alloy actuator: design and application in the prosthetic hand. in: *27th Annual International Conference of the Engineering in Medicine and Biology Society (IEEE-EMBS 2005)*. Shanghai, China; p. 6900–3, 2005.
23. Riccio, A., Saputo, S., Sellitto, A. Attuatore Bistabile. *UiBM Patent* 102020000025483; 16/11/2022.
24. Riccio, A., Napolitano, C., Sellitto, A., Acanfora, V., & Zarrelli, M. Development of a combined micro-macro mechanics analytical approach to design shape memory alloy spring-based actuators and its experimental validation. *Sensors*, 21(16), 5506, 2021.
25. Riccio, A., Saputo, S., Zarrelli, M., Sellitto, A., Napolitano, C., & Acanfora, V. Shape Memory Alloy-based actuator: Experimental and modelling. In *2021 IEEE 8th International Workshop on Metrology for AeroSpace (MetroAeroSpace)* (pp. 665-671). IEEE, 2021.